analytical chemistry

Article

pubs.acs.org/ac

Performance of a New 235 nm UV-LED-Based On-Capillary Photometric Detector

Yan Li,[†] Pavel N. Nesterenko,[†] Brett Paull,[†] Roger Stanley,[‡] and Mirek Macka*[,†]

[†]School of Physical Sciences and Australian Centre for Research on Separation Science (ACROSS), University of Tasmania, Hobart 7001, Australia

[‡]Centre for Food Innovation, University of Tasmania, Locked Bag 1370, Launceston 7250, Australia

Supporting Information

ABSTRACT: In this work, for the first time, a sub-250 nm light-emitting diode (LED) is investigated as a light source for optical detection in chemical analysis. A 235 nm deep ultraviolet-light-emitting diode (UV-LED) is employed within an on-capillary photometric detector and applied in capillary ion-exchange chromatography (IEC) for the detection of common ultraviolet (UV)-absorbing anions (here, iodide, nitrate, and nitrite). This investigation focused on fundamental properties of UV-LEDs, in particular, emission spectra, radiometric power, effective heat dissipation with a passive heat sink, and energy conversion. The detection showed excellent linearity with stray light down to 0.6%, and an effective path length at 92% of the used capillary inner diameter. The analytical performance parameters were demonstrated by detection of chromatographic separation of iodide in simulated seawater, showing a limit of detection (LOD) of 1.30 μmol L^{-1}, a linear range of 7.9−3937 μmol L^{-1}, and reproducibility (with a relative standard deviation (RSD)) of 0.6% for peak height 0.7% for peak area. In addition, nitrite and nitrate were selected to study the potential of using deep UV-LEDs as the light source in photometric detection for even lower-wavelength-absorbing analytes (λ_{max} = 209 nm for nitrite and 200 nm for nitrate), showing reproducibility (RSD = 1.2% and 3.6% for peak height and 0.9% and 2.9% for peak area, respectively) and LOD = 7 and 26 μmol L^{-1}.

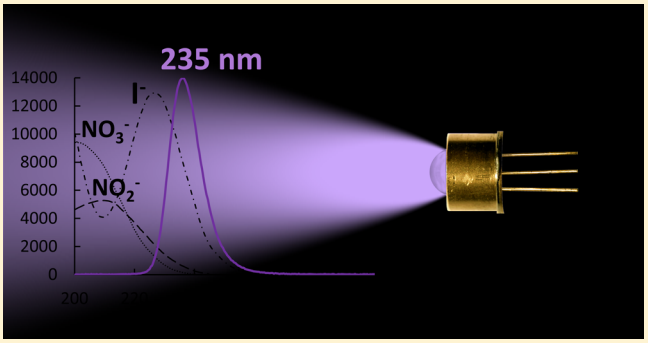

Over the last few decades, light-emitting diodes (LEDs) as light sources for chemical analysis and sensing have gained considerable attention,[1−3] as they indeed have in all areas of electronics and everyday consumer items. Within analytical optical instrumentation, since the first report by Flaschka et al. in 1973,[4] LEDs have played an increasingly important role, especially for absorbance and fluorescence measurements in various mostly miniaturized analytical and separation platforms. Early works (up to the 1990s) used LEDs in the visible spectral region[5−14] while works using ultraviolet-light-emitting diodes (UV-LEDs) appear sporadically from the 2000s.[15−26] In absorbance measurements, the high output intensity and low inherent noise make LEDs ideal quasi-monochromatic light sources, with numerous other advantages over conventional light sources.[2] When LEDs are applied as light sources within optical detectors, complex monochromators or optical filters are generally not necessary, because the desired emission wavelength of LEDs are emitted in a relatively narrow emission band (usually a bandwidth of 20−25 nm). These features provide for lower limits of detection (LODs), often comparable with, or indeed below that of detectors based upon conventional sources,[12,27,28] while also offering extended lifetimes, increased portability, and significantly lower costs. Other advantages of LEDs include low temperature fluctuations, mechanical stability, and relatively low power consumption. Two comprehensive reviews on LEDs for analytical applications have recently been published.[2,3]

LEDs emitting within the deep UV range (<300 nm) have a much wider span of applicability for analytical purposes, as most organic molecules have maximum absorptivity within the UV range, and the spectral area below 250 nm accesses a broader range of absorbers.[29] For deep UV-LEDs, the technology is mainly based on Group III nitride semiconductor materials, which normally includes crystalline alloys of aluminum nitride (AlN) and gallium nitride (GaN).[30] The bandgap energies of these end-point compounds are 3.43 eV for GaN and 6.04 eV for AlN at room temperature. Therefore, theoretically, by changing the content ratio of Ga and Al in the semiconductor material, with increased aluminum content leading to lower wavelengths, a 200−300 nm wavelength range can be achieved. Thanks to rapid advances in material sciences, deep UV-LEDs capable of delivering high optical output power are now emerging from the research laboratory.[31−33] However, the first application of deep UV-LEDs for absorbance

Received: July 23, 2016
Accepted: September 5, 2016
Published: September 5, 2016

DOI: 10.1021/acs.analchem.6b02832
Anal. Chem. 2016, 88, 12116−12121

photometric detection in liquid chromatography and other separation techniques was only relatively recently reported by Schmid et al. in 2008.[17] Since then, several other studies of optical detectors based on 255 and/or 280 nm deep UV-LEDs have been reported, including for capillary electrophoresis (CE),[18,23] high-performance liquid chromatography (HPLC),[34,35] narrow bore HPLC, and capillary HPLC.[21,22,24,25,36] However, in all of the above works, the source was a 255 nm UV-LED, which is on the upper limit of the useful range for many analytical applications.

This work reports the first use of a deep UV-LED with a peak emission wavelength of 235 nm for photometric detection, as well as its application within an on-capillary detector. The novel 235 nm deep UV-LED was investigated in an experimental design modified from a previous on-capillary detector successfully used with a number of visible (vis) and deep UV-LEDs.[18,28,36] The effect of emission spectrum, effective heat dissipation with a passive heat sink, radiometric power (also termed optical output power), and power conversion, on resulting detection performance were studied. Its analytical performance parameters were demonstrated as an on-capillary detector for capillary ion chromatography, and the detection of iodide in simulated seawater. In addition, nitrite and nitrate, which have maximum absorption wavelengths (λ_{max}) of 209 and 200 nm,[37−39] respectively, were selected to demonstrate the analytical potential of deep UV-LEDs for analytes absorbing at even lower wavelengths. The demonstrated examples showed, for the first time, analytes absorbing below 250 nm being directly detected using a photometric detector with LED as a light source.

2. EXPERIMENTAL SECTION

2.1. Chemicals and Reagents. Analytical or higher-grade reagents and deionized water (Millipore, Bedford, MA, USA) were used to prepare all solutions. Potassium hydroxide (KOH) eluent was electrolytically generated with a Dionex ICS-5000 Eluent Generator (Thermo Scientific, Sunnyvale, CA, USA) that was equipped with an EGC-MSA cartridge. Potassium nitrite, sodium sulfate, and potassium bromide were purchased from BHD Chemical Ltd. (Poole, English). Potassium nitrate was obtained from AJAX Chemicals Ltd. (Sydney, Australia). Orange G was obtained from Fluka (Buchs, Switzerland). Sodium chloride, boric acid, sodium bicarbonate, sodium hydroxide, and potassium iodide were sourced from Sigma−Aldrich (St. Louis, MO, USA). Potassium chloride was purchased from Griffin Certified Reagent (London, England). Sodium fluoride was sourced from R.P. Normapur AR (Paris, France).

Simulated seawater was prepared by dissolving 24.29 g of sodium chloride, 4.01 g of sodium sulfate, 0.6 g of potassium chloride, 0.21 g of sodium bicarbonate, 0.1 g of potassium bromide, 0.03 g of boric acid, and 0.002 g of sodium fluoride in 1037.33 g of deionized water, in accordance with the concentrations recommended within the method of Kester et al.,[40] with the exclusion of magnesium chloride, calcium chloride, and strontium chloride. All the stock solutions were prepared in deionized water. The stock solutions were stored at 4 °C. Working standards were prepared with an appropriate dilution of the stock solutions in deionized water. These solutions were prepared fresh weekly and stored at 4 °C when not in use.

2.2. Instrumentation. The 235 nm deep UV-LED was obtained from Crystal IS (Green Island, NY, USA). The LED-based photometric detector was assembled as an on-capillary device (polyimide (PI)-coated fused silica; 100 μm inner diameter (ID) from Polymicro Technologies, Phoenix, AZ, USA; with a detection window created by burning a small portion of the PI coating off the capillary). The detector employed an Agilent optical interface (Alignment interface, extended 50 μm coded red, from Agilent Technologies, Waldbronn, Germany) housed within an in-house designed aluminum holder, modified from a previous on-capillary detector design introduced and described in detail earlier.[18,28] The newly designed holder has an additional function as a heat sink (Figure 1). The LED light source was fixed on each side of the holder, being aligned with the detection window of the capillary. A controlling unit was employed, the details of which can be found in Johns et al.[28] In brief, this controlling unit contained a feedback circuit, which provided an output voltage proportional to the incident light level. This output voltage from the feedback circuit was then transferred into an offset circuit through a logarithmic amplifier (LOG101 integrated circuit; Burr-Brown, Tucson, AZ, USA). The offset circuit allowed the output level to be adjusted to any desired value. The resultant output absorbance was finally transferred into an eDAQ e-corder data acquisition system (Model ED401, Denistone East, New South Wales, Australia), which interfaced the LED detector and the eChart software as the data acquisition unit. A broadband SiC-based hybrid UV photodetector (containing a photodiode and an amplifier) (Model TOCON_ABC2; Sglux SolGel Technologies GmbH, Berlin, Germany) was used for detection. The LED was powered by a constant current power supply.

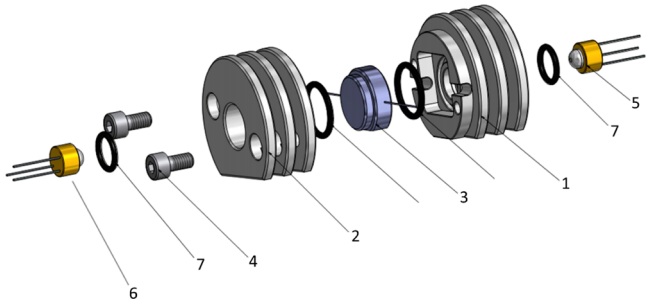

Figure 1. Design of the on-capillary photometric detection with heat sink function. Legend: (1) aluminum housing for LED; (2) aluminum housing for photodiode; (3) optical alignment interface, 50 μm slit;[28] (4) broached socket head cap screw; (5) LED; (6) photodiode; and (7) O-ring for sealing the cell.

The spectrum of the 235 nm LED was measured using an OceanOptics Model USB2000+XR1-ES miniature fiber-optic-based spectrometer (OceanOptics, Adelaide, Australia) with the integration time set at 8 ms. The optical output power was measured with a silicon photodiode (active area = 100 mm^2; Edmund Optics, York, U.K.), using its optical vs electric power calibration graph. A thermal imaging camera (Model E40, FLIR, Wilsonville, OR, USA) was employed for the LED temperature study. A UV/vis spectrophotometer (Model SP-8001, Metertech, Taipei, Taiwan, China) was used to measure the absorption spectrum of Orange G in water, using a 10 mm quartz cell.

A Dionex Model ICS-5000 ion chromatograph (Thermo Fisher Scientific, Sunnyvale, CA, USA) was used. The instrument was equipped with a dual pump (DP) configured

DOI: 10.1021/acs.analchem.6b02832
Anal. Chem. 2016, 88, 12116−12121

for capillary chromatography and for analytical chromatography, an eluent generator module electrolytically generating a high-purity KOH eluent from deionized water using a EGC-KOH cartridge, an IC Cube module, which included an injection valve (four-port internal 0.4 μL loop or six-port external 4 μL sample loop), a degassing cartridge, column heater, Dionex IonPac capillary columns (AS26 and AS19; 0.4 mm × 250 mm), and a carbonate removal device (CRD 200). The samples were injected via a Dionex AS-AP Autosampler (Thermo Fisher Scientific, Sunnyvale, CA, USA). Data was recorded at 20 Hz sampling frequency. The presented chromatograms were processed online by mains digital filter (50 Hz) and a low-pass digital filter with a cutoff frequency of 0.3 Hz, with negligible effect on peak heights.

2.3. Effective Path Length and Stray Light Measurement Procedure. Orange G was used as an absorbing probe to measure the on-capillary detector linearity as an absorbance-to-concentration relationship, which was then converted to a sensitivity (absorbance divided by concentration) versus absorbance plot.[9] The capillary was first flushed with water or the Orange G standard solution (~10 capillary volumes), then the flow was stopped and the absorbance was measured under static conditions. Each test solution was measured in triplicate and in order of increasing concentration. From the sensitivity vs absorbance curve, the effective path length and percentage of stray light values were calculated.[9]

3. RESULTS AND DISCUSSIONS

3.1. Emission Spectrum. The emission spectrum of the used LED is a key parameter showing not only the maximum wavelength and width of the emission band, but also the presence (or absence) of any other undesirable parasitic emission bands.[17,18,25] The emission spectrum for the 235 nm deep UV-LED (Table 1) shown in Figure 2A shows an

Table 1. Deep UV-LED Parameters

parameter	value
emission maximum, Em_{max}	236 nm
optical power, $P_{optical}$	0.052 mW
electrical power, $P_{electric}$	1030 mW
energy conversion rate	0.005%
expected release year	2017

important favorable feature. Unlike other previously used deep UV-LEDs in the 250 nm range,[17,18,25] this new type of 235 nm UV-LED produced only a negligible amount of parasitic emission light (<1%, Figure 2A) at higher wavelengths, particularly in the visible spectral region. This is due to the use of aluminum nitride (AlN) as the LED substrate material,[41] while the older type of deep UV-LEDs used sapphire-based substrates.[42] The new AlN substrate caused fewer lattice mismatches between the substrate and the AlN layers, which delivers superior properties, including increased lifetimes, higher output power,[43] and lower parasitic emission bands. Herein, because of the quasi-monochromatic emission spectra, which is relatively free of parasitic emission bands, an additional band-pass interference filter did not have to be included in the detection design, thus simplifying the design, and lowering cost and size. The emission bandwidth (half-height) of 13 nm implies that this deep UV-LED can be used to detect species absorbing significantly below 230 nm. Demonstrated herein for iodide, nitrite, and nitrate, with λ_{max} = 226 nm,[38,44] 209 nm,[37,39]

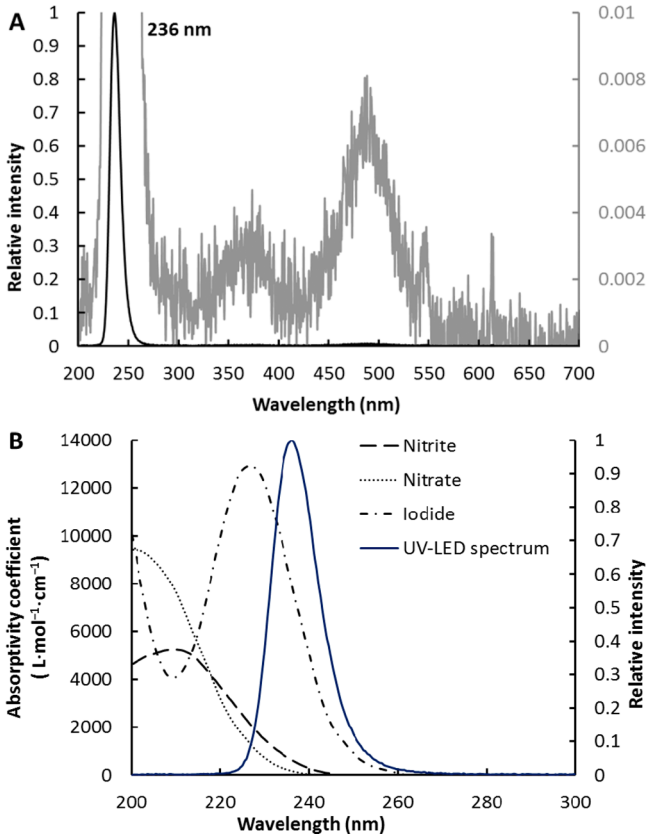

Figure 2. (A) Emission spectrum of the 235 nm UV-LED, with an emission bandwidth (half-height) of 13 nm. i = 100 mA. The gray line shows the relative intensity of the parasitic emission band is <1% of the intensity of desirable deep UV band. (B) UV spectra of iodide, nitrite, and nitrate overlaid with the 235 nm deep UV-LED emission spectrum. The analyte UV absorption spectra bands extend further to longer wavelength, which is partially covered by the LED emission spectrum. The UV absorption spectra of iodide, nitrite, and nitrate are adapted and calculated from previously reported results.[37−39,44] (Conditions: Passive heat sink; for more details, see the Experimental Section.)

and 200 nm,[37,39] respectively, although with absorption spectra extending into the 230 nm region (see spectra in Figure 2B). To date, UV-LED-based absorption detection have not been possible for the direct detection of such solutes.

3.2. Energy Conversion. A vital parameter of an LED is the optical output power. This parameter is dependent on the overall energy conversion of the LED (also termed external quantum efficiency), which, in turn, determines the heat production. Deep UV-LEDs have relatively low optical power output, compared to LEDs in the visible range,[2] and the heating phenomenon of deep UV-LEDs is well-known.[2,18,45] The LED lifetime, the emission wavelength, and the intensity at high current densities is negatively affected with increasing temperature;[45,46] therefore, here, it was necessary to investigate the impact of heating herein. It is noteworthy to mention that, although a heat sink is normally recommended by the manufacturer for deep UV-LEDs, a heat sink function was not included in any of the LED photometric detectors when using 255 and/or 280 nm deep UV-LEDs.[18,21,25,36] However, this study is the first demonstration of a high-power 235 nm deep UV-LED as a light source for optical detection, and therefore the impact of heating was studied. Temperature measurements showed that the body of the LED (measured at

DOI: 10.1021/acs.analchem.6b02832
Anal. Chem. 2016, 88, 12116−12121

the outer surface of the integrated lens) without the presence of an additional heat sink increased to above 80 °C (ambient temperature = 22.5 °C) within 7 min (Figure 3), while the LED

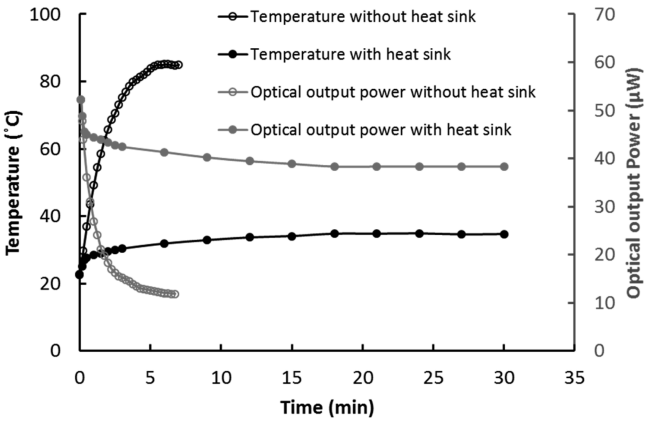

Figure 3. Body temperature and the optical output of the deep UV-LED with/without the heat sink (ambient temperature, 22.5 °C). Conditions: I = 100 mA; for more details, see the Experimental Section. Examples of thermal images are shown in the Supporting Information (Figure S1).

optical power decreased by 77%. Previous studies have shown that the half-life of deep UV-LEDs under ambient temperatures above 75 °C dropped to below 7% of that observed at room temperature.[45] Therefore, a heat sink is essential for maintaining high light intensity and preservation of the LED lifetime. An in-house designed and fabricated passive aluminum heat sink was employed, details of which can be found in the Experimental Section and in Figure 1. With the heat sink employed, the LED body temperature increase was considerably reduced and was maintained at ca. 33 °C (at ambient temperature, 22.5 °C). The subsequent LED optical output only decreased by 27% (Figure 3). After the temperature became steady (after ca. 15 min, see Figure 3), the light output was stable within ±1%.

The optical power emitted was measured as 0.052 mW, which is comparable with manufacturer's data (0.03−0.07 mW) for deep UV-LED around 245 nm.[47] While Sharma et al.[25] have shown that an additional focusing lens between a UV-LED and the slit can increase the light energy beneficial to low levels of baseline noise, in this work, we focused on a simple optical design without an additional focusing lens, as reported in our previous works.[18,28] The optical power of the 235 nm deep-UV LEDs is obviously satisfactory (photometric detector gives baseline noise at 30 μAU, as discussed in Section 3.3) in maintaining the level of light energy through the capillary and at the detector, thus maintaining acceptably low levels of noise, while keeping the detector design simple, compact, and inexpensive. The energy conversion was determined as the ratio of the optical power emitted and the input electrical power, at 1.03 W, delivered at the same time under the same conditions (see Table 1). Thus, the calculated energy conversion was 0.005%, which is a value much lower than for most Vis-LEDs, implying that this new deep UV-LED, although comparing favorably with other deep UV-LEDs in both optical power and an emission spectrum free of parasitic bands, has an unfavorable energy conversion ratio (with resulting heat generation).

3.3. Detection Performance Study and Demonstration as Photometric Detector in Capillary Chromatography. Detection performance, in terms of linearity, effective path length, and stray light, can be experimentally determined using a strongly absorbing compound at the detection wavelength, as demonstrated in the many of the previous works.[9,48,49] Here, Orange G was chosen as the test absorbing compound, because it absorbs strongly at 235 nm. Detection linearity was measured and plotted as detection sensitivity (AU/mol L^{-1}) vs absorbance graphs (see Figure 4). This graph

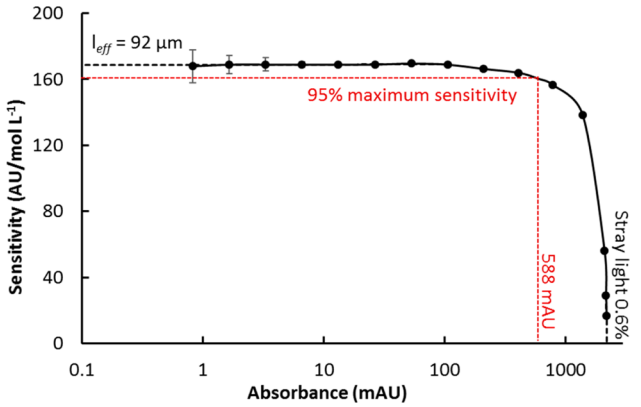

Figure 4. Detection linearity depicted as a sensitivity vs absorbance (A) graph. Conditions: Capillary inner diameter, 100 μm; test analyte, Orange G; effective path length, l_{eff} = 92 μm, calculated for sensitivity extrapolated to A = 0 equal to 162 AU/mol L^{-1}, and orange G absorptivity = 18,300 cm L mol^{-1} as measured. The stray light % from the extrapolated high end of the curve at A = 2.206. An upper limit of detection (LOD), determined as the absorbance corresponding to 95% sensitivity, was calculated as 588 mAU (see marks in red).

allows direct evaluation of the level of stray light and the effective path length. The absorbance at which the sensitivity decreased by 5% from its maximum value was used to define the upper limit of detector linearity.[49] The effective path length was measured as 92 μm, which is 92% matched with the 100 μm capillary ID and comparable with commercial on-capillary photometric detectors (66%−100% matched with the inserted capillary ID).[48] In principle, the stray light consists of two contributions, namely, the light passing through the capillary wall without passing through the capillary lumen with the absorbing liquid, as well as a degree of polychromacity of the LED light. The level of stray light was determined to be only 0.62%, compared to 30.5% for a previous study using a 254 nm LED.[17,18,25] The upper limit of detection (LOD) linearity of 588 mAU was calculated, as shown in Figure 4 (however, the dynamic linear range extends up to ca. 2 AU). This is comparable with the upper detector linearity limit of a commercial Agilent ^{3D}CE system (785 mAU[27]), based on a deuterium lamp and diode array detector, and significantly higher than previous results with deep UV-LED light sources, which were typically lower than 100 mAU.[18,23] Overall, the determined detection design parameters—namely, linearity, effective path length, and stray light—were superior to comparable designs used in the past.[18,27,28]

As a potential application of the new deep UV-LED-based detector, its application as a direct photometric detector for the detection of iodide, following its separation in simulated seawater using capillary ion chromatography, was examined (see Figure 5A). Iodide analysis in seawater is of considerable

DOI: 10.1021/acs.analchem.6b02832
Anal. Chem. 2016, 88, 12116−12121

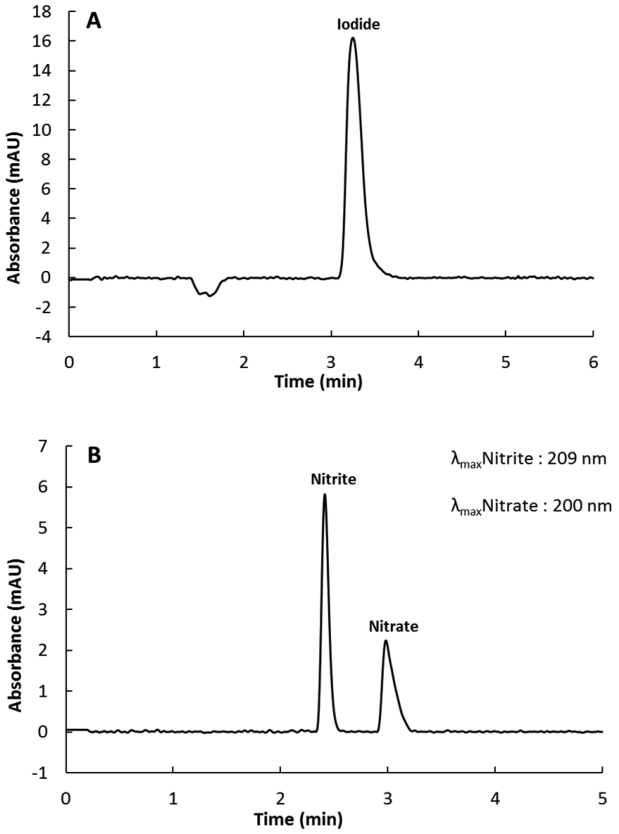

Figure 5. (A) Isocratic separation of iodide (197 μmol L^{-1}) in simulated seawater using capillary IEC. Conditions: eluent, 100 mM KOH; 500 mM sodium chloride; flow rate, 20 μL min^{-1}; column, IonPac AS26 capillary column (0.4 mm × 250 mm); injection volume, 4 μL. (B) Isocratic separation of nitrite (0.43 mmol L^{-1}) and nitrate (0.65 mmol L^{-1}) using capillary IEC. Conditions: eluent, 40 mM KOH; flow rate, 15 μL min^{-1}; column, IonPac AS19 capillary column (0.4 mm × 250 mm); injection volume, 0.4 μL. Detection: 235 nm deep UV-LED photometric detection. For more details, see the Experimental Section. Maximum absorption wavelength (λ_{max}) of nitrite and nitrate according to previously reported data.[37,39]

interest to the marine biology community, as well as in various other biomedical and environmental matrices.[50−53] The isocratic ion chromatographic method applied here was based on a standard matrix-elimination technique,[52,54,55] formally applied with direct UV detection at 226 nm to avoid interference due to a large excess of chloride.[56] Detection using the 235 nm deep UV-LED-based detector revealed satisfactory performance, with baseline noise determined under these conditions as only 30 μAU, which is comparable with previously reported results (4.4−250 μAU) using UV-LEDs as light source for photometric detection.[11,18,21,23,25,35] The detector under real chromatography conditions gave satisfactorily low levels of baseline noise, while further improvement can be made through the use of software averaging, which incorporates the analogue low-pass filter, such as that employed by Sharma et al.[25] The LOD of iodide in simulated seawater under these conditions was determined to be 1.30 μmol L^{-1}. A linear range based on peak areas of 7.9−3937 μmol L^{-1} was achieved (see Figure S2 in the Supporting Information). The reproducibility of peak heights and peak area was represented by relative standard deviations (RSDs) of 1.3% and 1.0%, respectively, confirming satisfactory separation and detection performance. Because of the negligible absorbance of chloride at 235 nm, the detector baseline only increased by 5.8 mAU, when the eluent was changed from 5 mM KOH, to 500 mM sodium chloride and 100 mM NaOH, and this shift was likely to be partially caused by a change in refractive index. The LOD value for iodide in simulated seawater was 11−137 times higher than those reported previously with comparable injection volumes[51,53,55,57] and 226-nm *z*-cell UV detection. However, given that the on-capillary detection used here provided an effective path length that was ∼100 times shorter than a typical commercial *z*-type flow cell, and the detection emission peak wavelength is 10 nm further away from the λ_{max} of iodide (226 nm, Figure 2B), these results are not only satisfactory, they are extremely encouraging.

Further application of the detector to the detection of nitrite and nitrate (separated again using capillary IC) highlighted the potential of using a deep UV-LED for solutes that have λ_{max} < 220 nm (Figure 5B). In this instance, the LODs were 7 and 26 μmol L^{-1} for nitrite and nitrate, respectively. The reproducibility of peak heights was 1.2% and 3.6%, and peak areas are 0.9% and 2.9% RSD for nitrite and nitrate, respectively. As expected, the LODs of nitrite and nitrate were somewhat inferior to those previously reported using direct UV photometric detection,[58] obviously because of the mismatch between the 235 nm deep UV-LED emission and λ_{max} value of nitrite (209 nm) and nitrate (200 nm)[37,39] (see Figure 2B). However, this application showed, for the first time, the detection of nitrite and nitrate by a direct deep UV-LED detector in a microfluidic analytical application, and thus showcasing the greater potential for deep UV-LEDs in analytical chemistry.

4. CONCLUSIONS

This study shows the first application of a deep UV-LED emitting wavelength under 250 nm as a light source for photometric detection in chemical analysis, and it illustrates the potential that deep UV-LEDs obviously have as light sources for photometric detection in robust, miniaturized, low-cost analytical devices. The performance of the 235 nm deep UV-LED was found to be overall satisfactory and promising, with particular regard to its emission spectra free of parasitic emissions, optical output, and low level of stray light and high upper limit of detector linearity when applied within an on-capillary detector. Specific observations from this investigation point attention to the issue of extensive heating, which must be overcome for the current generation of deep UV-LEDs to gain wider application. Herein, a passive heat sink offered a straightforward solution, preventing a loss of ca. 50% of the light intensity due to overheating. Ongoing work is now focusing on combining this 235 nm deep UV-LED with a *z*-type flow cell, which will potentially increase the detection sensitivity 10−100 fold.

■ ASSOCIATED CONTENT

Supporting Information

The Supporting Information is available free of charge on the ACS Publications website at DOI: 10.1021/acs.analchem.6b02832.

Graphical depiction of temperature measurement using thermal imaging; calibration curve of determination of iodide in simulated seawater (PDF)

DOI: 10.1021/acs.analchem.6b02832
Anal. Chem. 2016, 88, 12116−12121

AUTHOR INFORMATION

Corresponding Author

*E-mail: Mirek.Macka@utas.edu.au Tel.: +61 362266670. Fax: +61 362262858.

Notes

The authors declare no competing financial interest.

ACKNOWLEDGMENTS

Crystal IS is acknowledged for their donation of the 235 nm LED. Christopher Broinowski is acknowledged for helping to construct the passive heat sink. Miloš Dvořák is acknowledged for providing the UV absorbance measurement of Orange G. Estrella Sanz Rodriguez is acknowledged for providing the simulated seawater. M.M. gratefully acknowledges the Australian Research Council Future Fellowship (No. FT120100559).

REFERENCES

(1) Dasgupta, P. K.; Eom, I.-Y.; Morris, K. J.; Li, J. *Anal. Chim. Acta* **2003**, *500*, 337−364.
(2) Macka, M.; Piasecki, T.; Dasgupta, P. K. *Annu. Rev. Anal. Chem.* **2014**, *7*, 183−207.
(3) Bui, D. A.; Hauser, P. C. *Anal. Chim. Acta* **2015**, *853*, 46−58.
(4) Flaschka, H.; Mckeithan, C.; Barnes, R. *Anal. Lett.* **1973**, *6*, 585−594.
(5) Betteridge, D. *Anal. Chem.* **1978**, *50*, 832A−846A.
(6) Betteridge, D.; Dagless, E.; Fields, B.; Graves, N. *Analyst* **1978**, *103*, 897−908.
(7) Pawliszyn, J. *Rev. Sci. Instrum.* **1987**, *58*, 245−248.
(8) Trojanowicz, M.; Worsfold, P.; Clinch, J. *TrAC, Trends Anal. Chem.* **1988**, *7*, 301−305.
(9) Macka, M.; Andersson, P.; Haddad, P. R. *Electrophoresis* **1996**, *17*, 1898−1905.
(10) Boring, C. B.; Dasgupta, P. K. *Anal. Chim. Acta* **1997**, *342*, 123−132.
(11) Butler, P. A. G.; Mills, B.; Hauser, P. C. *Analyst* **1997**, *122*, 949−953.
(12) Macka, M.; Paull, B.; Andersson, P.; Haddad, P. R. *J. Chromatogr., A* **1997**, *767*, 303−310.
(13) Macka, M.; Nesterenko, P.; Andersson, P.; Haddad, P. R. *J. Chromatogr., A* **1998**, *803*, 279−290.
(14) Macka, M.; Nesterenko, P.; Haddad, P. R. *J. Microcolumn Sep.* **1999**, *11*, 1−9.
(15) King, M.; Paull, B.; Haddad, P. R.; Macka, M. *Analyst* **2002**, *127*, 1564−1567.
(16) Xiao, D.; Zhao, S.; Yuan, H.; Yang, X. *Electrophoresis* **2007**, *28*, 233−242.
(17) Schmid, S.; Macka, M.; Hauser, P. C. *Analyst* **2008**, *133*, 465−469.
(18) Krcmova, L.; Stjernlof, A.; Mehlen, S.; Hauser, P. C.; Abele, S.; Paull, B.; Macka, M. *Analyst* **2009**, *134*, 2394−2396.
(19) Ryvolová, M.; Preisler, J.; Foret, F. e.; Hauser, P. C.; Krásenský, P.; Paull, B.; Macka, M. *Anal. Chem.* **2010**, *82*, 129−135.
(20) Xiao, D.; Yan, L.; Yuan, H.; Zhao, S.; Yang, X.; Choi, M. M. *Electrophoresis* **2009**, *30*, 189−202.
(21) Bui, D. A.; Bomastyk, B.; Hauser, P. C. *J. Sep. Sci.* **2013**, *36*, 3152−3157.
(22) Sharma, S.; Plistil, A.; Simpson, R. S.; Liu, K.; Farnsworth, P. B.; Stearns, S. D.; Lee, M. L. *J. Chromatogr., A* **2014**, *1327*, 80−89.
(23) Bui, D. A.; Hauser, P. C. *J. Chromatogr., A* **2015**, *1421*, 203−208.
(24) Sharma, S.; Plistil, A.; Barnett, H. E.; Tolley, H. D.; Farnsworth, P. B.; Stearns, S. D.; Lee, M. L. *Anal. Chem.* **2015**, *87*, 10457−10461.
(25) Sharma, S.; Tolley, H. D.; Farnsworth, P. B.; Lee, M. L. *Anal. Chem.* **2015**, *87*, 1381−1386.
(26) Bui, D. A.; Hauser, P. C. *Sens. Actuators, B* **2016**, *235*, 622−626.
(27) Johns, C.; Macka, M.; Haddad, P. R. *Electrophoresis* **2003**, *24*, 2150−2167.
(28) Johns, C.; Macka, M.; Haddad, P. R. *Electrophoresis* **2004**, *25*, 3145−3152.
(29) Korshin, G. V.; Li, C.-W.; Benjamin, M. M. *Water Res.* **1997**, *31*, 1787−1795.
(30) Nishida, T.; Saito, H.; Kobayashi, N. *Appl. Phys. Lett.* **2001**, *78*, 399−400.
(31) Zhang, J.; Chitnis, A.; Adivarahan, V.; Wu, S.; Mandavilli, V.; Pachipulusu, R.; Shatalov, M.; Simin, G.; Yang, J.; Khan, M. A. *Appl. Phys. Lett.* **2002**, *81*, 4910−4912.
(32) Zhang, J. P.; Hu, X.; Bilenko, Y.; Deng, J.; Lunev, A.; Shur, M. S.; Gaska, R.; Shatalov, M.; Yang, J. W.; Khan, M. A. *Appl. Phys. Lett.* **2004**, *85*, 5532−5534.
(33) Allerman, A.; Crawford, M.; Fischer, A.; Bogart, K.; Lee, S.; Follstaedt, D.; Provencio, P.; Koleske, D. *J. Cryst. Growth* **2004**, *272*, 227−241.
(34) Kraiczek, K. G.; Bonjour, R.; Salvadé, Y.; Zengerle, R. *Anal. Chem.* **2014**, *86*, 1146−1152.
(35) Bomastyk, B.; Petrovic, I.; Hauser, P. C. *J. Chromatogr., A* **2011**, *1218*, 3750−3756.
(36) Li, Y.; Dvorak, M.; Nesterenko, P. N.; Stanley, R.; Nuchtavorn, N.; Krcmova, L. K.; Aufartova, J.; Macka, M. *Anal. Chim. Acta* **2015**, *896*, 166−176.
(37) Maslakowez, I. *Eur. Phys. J. A* **1928**, *51*, 696−706.
(38) Chen, S.-L.; Wang, S.; Lucia, L. A. *J. Colloid Interface Sci.* **2004**, *275*, 392−397.
(39) Sung, W. *J.—Am. Water Works Assoc.* **2011**, *103*, 97−103.
(40) Kester, D. R.; Duedall, I. W.; Connors, D. N.; Pytkowicz, Rm. *Limnol. Oceanogr.* **1967**, *12*, 176−179.
(41) http://www.cisuvc.com/products/optan.
(42) Shur, M.; Gaska, R. In *Proceedings of SPIE 2008*; Society of Photo-optical Instrumentation Engineers: Bellingham, WA, 2008; pp 6894191−6894198.
(43) Kneissl, M.; Kolbe, T.; Chua, C.; Kueller, V.; Lobo, N.; Stellmach, J.; Knauer, A.; Rodriguez, H.; Einfeldt, S.; Yang, Z.; Johnson, N. M.; Weyers, M. *Semicond. Sci. Technol.* **2011**, *26*, 26.
(44) Guenther, E. A.; Johnson, K. S.; Coale, K. H. *Anal. Chem.* **2001**, *73*, 3481−3487.
(45) Reed, M. L.; Wraback, M.; Lunev, A.; Bilenko, Y.; Hu, X.; Sattu, A.; Deng, J.; Shatalov, M.; Gaska, R. *Phys. Status Solidi C* **2008**, *5*, 2053−2055.
(46) Shur, M. S.; Gaska, R. *IEEE Trans. Electron Devices* **2010**, *57*, 12−25.
(47) http://www.qphotonics.com/Deep-UV-light-emitting-diode-30-70uW-240nm.html.
(48) Johns, C.; Macka, M.; Haddad, P. R.; King, M.; Paull, B. *J. Chromatogr., A* **2001**, *927*, 237−241.
(49) Johns, C.; Macka, M.; Haddad, P. R. *LC-GC Eur.* **2003**, *16*, 290.
(50) Smith, J. D.; Butler, E. C. V.; Airey, D.; Sandars, G. *Mar. Chem.* **1990**, *28*, 353−364.
(51) Mctaggart, A. R.; Butler, E. C. V.; Haddad, P. R.; Middleton, J. H. *Mar. Chem.* **1994**, *47*, 159−172.
(52) Ito, K. *J. Chromatogr., A* **1999**, *830*, 211−217.
(53) Rodriguez, E. S.; Setiawan, A. N.; Pope, S.; Haddad, P. R.; Nesterenko, P. N.; Paull, B. *Anal. Methods* **2016**, *8*, 5587−5595.
(54) Ito, K. *Anal. Chem.* **1997**, *69*, 3628−3632.
(55) Ito, K.; Sunahara, H. *J. Chromatogr.* **1990**, *502*, 121−129.
(56) Chandramouleeswaran, S.; Vijayalakshmi, B.; Kartihkeyan, S.; Rao, T. P.; Iyer, C. S. *Microchim. Acta* **1998**, *128*, 75−77.
(57) *Determination of thiosulfate in refinery and other wastewaters*; Application Note 239; Dionex, 2001.
(58) Connolly, D.; Paull, B. *Anal. Chim. Acta* **2001**, *441*, 53−62.

NOTE ADDED AFTER ASAP PUBLICATION

This paper was published on 9/26/2016. Additional text changes were made and the revised version was reposted on 9/29/2016.

DOI: 10.1021/acs.analchem.6b02832
Anal. Chem. 2016, 88, 12116−12121